Detectability Of Ultra-Faint Dwarf Galaxies With Gaia

Cecilia Mateu[1,2], Teresa Antoja[3], Luis Aguilar[1], Francesca Figueras[4], Anthony Brown[5], Erika Antiche[4], Fabiola Hernández-Pérez[2], Octavio Valenzuela[6], Antonio Aparicio[7], Sebastián Hidalgo[7], Héctor Velázquez[1]

(1) Instituto de Astronomía, Universidad Nacional Autónoma de México, Ensenada B.C., México (**cmateu@astrosen.unam.mx**)
(2) Centro de Investigaciones de Astronomía (CIDA), Mérida, Venezuela,
(3) ESA, European Space Research and Technology Centre (ESTEC), Noordwijk, The Netherlands
(4) Departament d'Astronomia i Meteorologia, Institut de Ciències del Cosmos, Universitat de Barcelona, Barcelona, Spain
(5) Sterrewacht Leiden, Leiden, the Netherlands, (6) Instituto de Astronomia, UNAM, México DF, México
(7) Instituto de Astrofísica de Canarias, Tenerife, Spain

ABSTRACT. We present a technique to detect Ultra-Faint Dwarf Galaxies (UFDs) in the Galactic Halo, using sky and proper motion information. The method uses wavelet transforms to detect peaks in the sky and proper motion planes, and to evaluate the probability of these being stochastic fluctuations. *We aim to map thoroughly the detection limits of this technique*. For this, we have produced a library of 15,000 synthetic UFDs, embedded in the Gaia Universe Model Snapshot (GUMS) background, each at a different distance, different luminosity, half-light radius, velocity dispersion and center-of-mass velocity, varying in ranges that extend well beyond those spanned by known classical and ultra-faint dSphs. We use these synthetic UFDs as a benchmark to characterize the completeness and detection limits of our technique, and present our results as a function of different physical and observable parameters of the UFDs.

I. INTRODUCTION.

Gaia will play a crucial role in the identification and study of substructure in the Galactic Halo. In particular, providing a census of Milky Way satellite galaxies with well understood detection limits and completeness is absolutely necessary to allow for a proper comparison between the observed distributions of galactic satellites and predictions from galaxy formation models.

II. THE DETECTION TOOLS.

Here we describe the procedure followed to identify possible UFD candidates, using sky and proper motion information.

In 2°x2° fields we search for overdensities in the l-b and μ_l-μ_b planes independently, using a Wavelet Transform (WT) algorithm (Starck & Murtagh 2002). We search for density peaks in four different WT scales in the l-b and μ_l-μ_b planes (Fig. 1) and keep only those peaks that have stars in common in both planes.

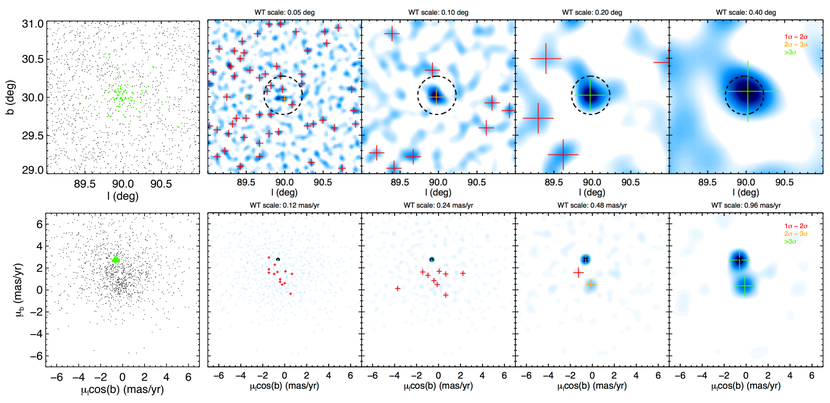

Figure 1. The top and bottom rows show the l-b and μ_l-μ_b planes respectively, around a mock UFD. Starting from the 2nd column, the corresponding WTs are shown from left to right for increasing scales. The dashed circle indicates the true position of the UFD.

We then evaluate the probability P_c that a given peak is due to stochastic fluctuations, as the Poisson probability of having observed N_c stars in common in both planes, when only $<N_c>$ are expected at random for a given WT scale. In each field we select detections with the smallest probability (i.e. less likely), which do not overlap within their corresponding WT scales. Finally, we compute the significance of a detection in terms of how many standard deviations is the observed N_c deviated from the expected number $<N_c>$.

III. THE BENCHMARK

The Galactic Background. The synthetic UFDs are embedded in the GUMS Galactic model background from Robin et al. (2012),

The UFD model. The synthetic galaxies are simulated as Plummer spheres with isotropic velocity distributions, characterized by their half-light radii r_h and velocity dispersion σ. The stellar population is simulated as a 12 Gyr-old burst, with metallicity [Fe/H]=-2 and total luminosity L_V, using the model from Hernández-Pérez & Bruzual (2013).

The selection function and error model. We assume all stars with G≤20 will be observable with Gaia, and simulate the observational errors using the latest post-launch science performance figures, using the publicly available code from Romero-Gómez et al. (2014)†. To reduce contamination from foreground disk dwarfs, we filter out stars with large surface gravity ($\log g$-$\Delta\log g$>4) and parallax (ϖ-$\Delta\varpi$>200μas, i.e. consistent with distance <5kpc) in the full simulated (UFD+GUMS) catalogue.

IV. THE SYNTHETIC UFD LIBRARY

Using these models (§. III) we have generated a library of 15,000 synthetic UFDs located at various distances with different total luminosity L_V, half-light radius r_h, velocity dispersion σ_v and center-of-mass velocity V_{gal}. Fig. 2 shows the parameter space explored by the UFD library (•), which extends well beyond the span of known classical (■) and ultra-faint dSphs (◆).

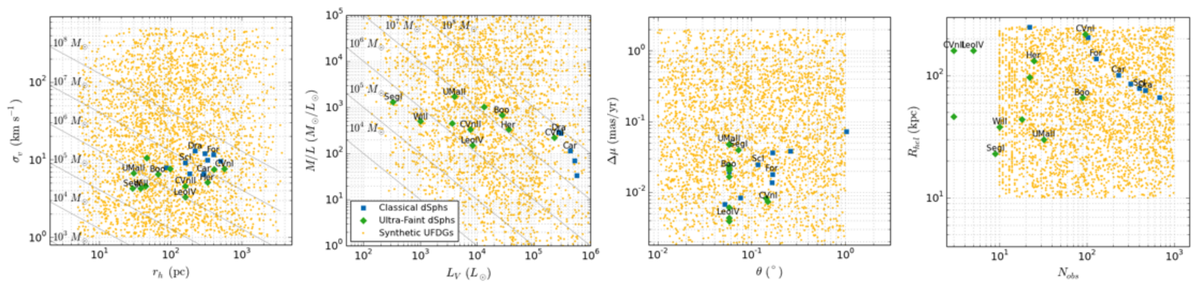

Figure 2. From left to right: velocity dispersion σ_v vs. half-light radius r_h, Mass-to-light ratio M/L vs. total luminosity L_V, apparent size in proper motion $\Delta\mu$ vs. apparent size in the sky $\Delta\theta$, and heliocentric distance R_{hel} vs. N_{OBS} the total number of stars in the UFD that will be *observable by Gaia* (assuming the stellar population model described in §. III).

V. DETECTABILITY LIMITS

Figure 3 shows the detection significance (color scale) in three different planes of physical parameters. In this set of experiments only the parameters shown in each plot are variable, while the others are kept constant (see figure caption). These illustrate, for simplified cases, the detection boundaries in terms of physical parameters. The left panel shows there is a marked dependence with r_h, so that more concentrated systems are more easily detected (at fixed R_{hel}); whereas there's almost no dependence with σ_v, because the apparent size in proper motion space is dominated by the errors. The middle panel shows the dependence with L_V, note that very faint systems (L_V≲5000$L_\odot$) are detectable up to ~30-60kpc.

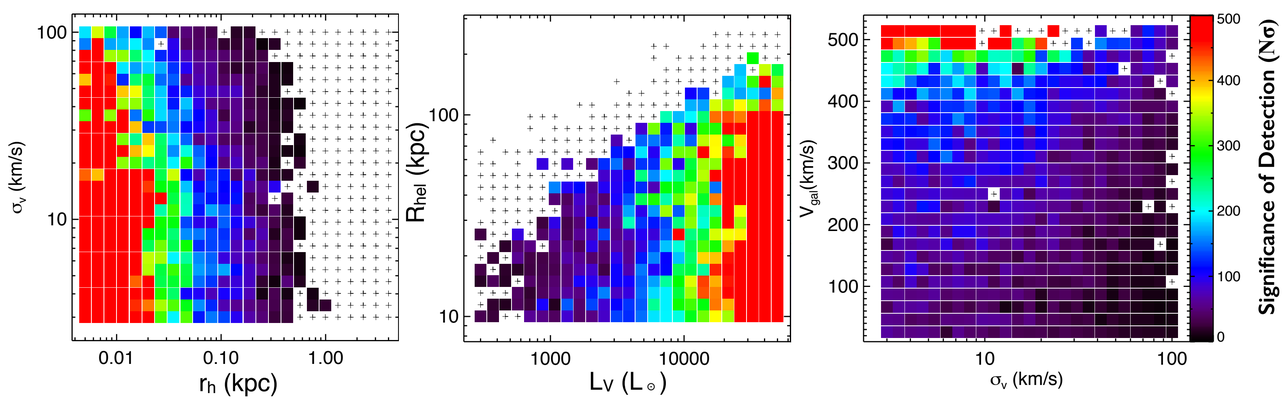

Figure 3. *Left*: σ_v vs. r_h, *Middle*: R_{hel} vs. L_V, *Right*: V_{gal} vs. σ_v. The color scale is proportional to the Nσ significance of detections, crosses (+) indicate non-detections. For these plots, we use a set of libraries in which only the parameters shown in each plot are variable (when fixed, the chosen values are: R_{hel}=20kpc, r_h=0.8kpc, σ_v=5km/s, L_V=5000$L_\odot$, V_{gal}=400 km/s).

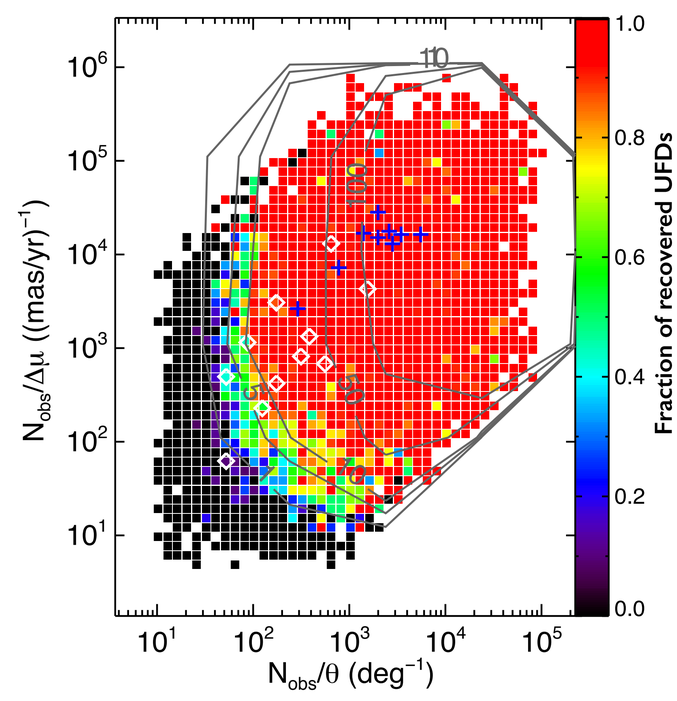

Figure 4. $N_{OBS}/\Delta\mu$ vs. $N_{OBS}/\Delta\theta$ for the full library of synthetic UFDs. The color scale shows the fraction of detected UFDs per bin. The significance of the UFD detections are illustrated by the labeled contours, which show 1σ, 5σ, 10σ, 50σ, 100σ levels. The diamonds (◇) and crosses (+) show the positions of the known UFD and classical dSphs respectively.

To find the detection limits of our method we explore a space of direct observables, since these are the quantities that effectively determine the statistical significance with which a galaxy can be detected.

Figure 4 shows a plot of the fraction of recovered UFDs (color scale) per bin in the $N_{OBS}/\Delta\mu$ vs. $N_{OBS}/\Delta\theta$ plane, for the full library described in §. IV. $N_{OBS}/\Delta\mu$ and $N_{OBS}/\Delta\theta$ represent (linear) number densities in the planes in which we conducted our search. The plot shows that as these densities increase, the detection significance increases (contours); as does the fraction of UFDs recovered (color scale). This fraction can be taken as a mean probability of detection for any UFD with a given value of $N_{OBS}/\Delta\mu$ and $N_{OBS}/\Delta\theta$ detection, and thus the plot in Fig. 4 can be used e.g. with cosmological models to produce mock UFDs samples that will be directly comparable with the UFD catalogue resulting from applying our method to Gaia data.

REFERENCES
Hernández-Pérez & Bruzual 2013, MNRAS 431, 2612
Robin et al. 2012, A&A, 543, A100
Romero-Gómez et al. 2014, MNRAS, in print (arxiv/1411.6389)
Starck & Murtagh 2002, Astronomical Image and Data Analysis, Springer

† https://github.com/mromerog/Gaia-errors